Materials Science Forum Vols. 783-786 (2014) pp 1913-1919

doi:10.4028/www.scientific.net/MSF.783-786.1913

Properties of indium tin oxide/amorphous alloys bi-layer films as transparent electrodes

H. K. Lin[1,a], K. C. Cheng[1,b], T. P. Cho[2,c] and J. C. Huang[3,d]

[1] Graduate Institute of Materials Engineering, National Pingtung University of Science and Technology, Pingtung 91201, Taiwan

[2] Metal Industries Research & Development Centre, Kaohsiung 821, Taiwan

[3] Department of Materials and Optoelectronic Science; Center for Nanoscience and Nanotechnology,

National Sun Yat-Sen University, Kaohsiung 804, Taiwan

[a]e-mail: HKLin@mail.npust.edu.tw, [b]e-mail: chen000790@gmail.com,
[c]e-mail:tpcho@mail.mirdc.org.tw, [d]e-mail: jacobc@faculty.nsysu.edu.tw

Keywords: AgMgAl, ZrCu, TCO, metallic glasses, bending test

Abstract

The amorphous alloy films of ZrCu and AgMgAl, layers deposited by co-sputtering was utilized as the metallic layer in the bi-layer structure transparent conductive electrode of ZrCu/ITO and AgMgAl/ITO deposited on the PET substrate using magnetron sputtering at room temperature. In the transmittance performance, the 30 nm ITO/3 nm ZrCu and 30 nm ITO/15 nm AgMgAl films could show the optical transmittance of 73 % and 70% at visible light of 550 nm wavelength and maintain the stable transmittance of 70~75% from visible light to infrared region. Meanwhile, the 30 nm ITO/9 nm ZrCu and the 30 nm ITO/15 nm AgMgAl films could show the better sheet resistance of 136 Ω/sq. and 135 Ω/sq. respectively. In addition, compared with the ITO film, the current metallic glasses were utilized as the metallic layer in the bi-layer structure transparent conductive electrode showed the better bending properties. The relative change of resistivity is below 0.4, significantly lower than that of the commercial PET/ITO product. The ZCI would exhibit lower variation in resistance owing to short crack propagated in the amorphous alloy of ZrCu layer after 10000 cycles bending test.

1. Introduction

Transparent conducting oxides (TCOs) are widely used in solar cells, optoelectronics, touch panel and flat panel displays [1-3]. In general, indium tin oxide (ITO) thin films as transparent conductive electrodes are widely used in different applications because of their low electrical resistance and high transmittance in the visible range of the spectrum [4, 5]. For the goal of getting better sheet resistance, the thickness of ITO thin film must reach to 100 nm [6, 7], but this would lead to a disadvantage owing to the high cost of indium. In order to decrease the use of ITO materials by reducing the thickness of ITO film, the transparent conductor films in thickness lower than 100 nm with the sandwich structure of ITO/metal layer/ITO have been verified the

performance of good conductivity and transparency in visible light range due to higher carrier concentration in the middle layer of metal film [8-12]. The metal materials of middle layer were generally silver or copper, some of highly conductive metals, and the optimal thickness of middle layer was about 8~12 nm to couple the good transmittance in visible light and higher conductivity. The thinner metal film (<8 nm) would exhibit worse conductivity due to the discontinuous film of island structure; however, the thicker and continuous metal film would result in the high reflectivity to lower the entire transmittance in visible spectrum because of the continuous film structure and higher plasma frequency of metal materials. The same sandwich structure could also get the similar optical and electrical performance in other transparent conducting oxide, for example, ZnO – Ag – ZnO [11] or ZnS – Ag – ZnS [13].

The interlayer of crystalline metal is typically required to be very thin (< 8 nm), so as not to degrade the optical transmission. However, it easily induces the poor electric conductivity due to the discontinuous film of the island structure. All common crystalline metal films in the extra-thin range of 3-6 nm are difficult to form flat and continuous films. Upon increasing to a film thickness over 10 nm, the thicker and continuous metal film would result in much lower and unaccepted transmittance in visible spectrum because of the continuous film structure and higher plasma frequency of metal materials. In addition, ITO film is inevitably stiff and brittle, whereas the flexible polymer substrate is not. It follows that the PET/ITO laminate, while subjected to tensile or fatigue loading, would be prone to tensile micro-cracks which in-turns leads to the increase of the ITO electrode resistivity and the degradation of optical transmission [14, 15].

Metallic glass is another category of metal materials. The extensive research on the bulk metallic glasses (BMGs) [16-19], thin film metallic glasses (TFMGs) have also been explored in recent years [20-22]. Among many TFMGs alloy system, ZrCu is the model binary metallic glass system, with a wide composition range for high glass forming ability and promising characteristics. In order to enhance the mechanical properties of the PET/ITO laminate, a thin ZrCu TFMG interlayer of the thickness of 3-12 nm was deposited, forming the PET/ZrCu/ITO hybrid structure [23]. This ZrCu film could form a continuous and flat interlayer even at the lowest thickness of 3-6 nm.

In this study, the bi-layer structures, consisting of a metallic-glass film and an outer layer of ITO, were chosen to prepare the transparent conductive film deposited on a flexible substrate of polyethylene terephthalate (PET). TFMGs alloy system included ZrCu and AgMgAl alloy was used as a metallic glass film. We also investigate the influence of metallic-glass film on optoelectronic properties of this transparent conductive electrode, and compare the difference with both bi-layer structure films. The fatigue properties of the bi-layer structure films, subject to three-point bending fatigue test, are examined and compared to commercial products.

2. Experimental

The flexible polymer PET substrate was purchased from DuPontTeijin (ST504), 125 μm thickness. The transmittance of PET is 88% at wavelength of 550 nm. Firstly, the TFMG was deposited onto the PET substrate by the sputtering method and then ITO was sputtered on the

TFMG film. The ITO target was with the composition of 90 wt% In_2O_3 and 10 wt% SnO_2 and the deposition conditions are listed in Table 1. The thickness of the ITO layer was fixed at 30 nm and that of the metallic films was varied from 3 to 12 nm. The morphology and components ratio of films were examined by scanning electron microscopy (SEM) with energy dispersive spectrometry (EDS). The sheet resistance was measured using a four-point probe technique. Optical transmittance and reflectivity were measured in the range of 200-1000 nm by UV-VIS-IR spectrophotometer (N&K analyzer 1280).The bending fatigue system can keep on bending the samples from plane to specific curvature radius for customized cycles setting and the variation of electrical resistivity was measured during the fatigue test. The bending fatigue specimen measures 45 mm in length, 10 mm in width, and 125 μm in thickness. The bending velocity was defined as 1 cycle/second, and the maximum fatigue bending curvature was varied from 15.5 mm to 19.5 mm.

3. Result and discussion

The optical transmittance of the PET/TFMG-AgMgAl and PET/AgMgAl/ITO is shown in Fig. 1, as a function of TFMG thickness. The transmittance of the 6 nm AgMgAl film on the PET substrate is ~60% in the visible wavelength of 550 nm but the transmittance would decline with increasing amorphous AgMgAl layer thickness, as shown in Fig. 1. After the ITO film was deposited on the metallic film, the transmittance of PET/AgMgAl 15 nm/ITO films will increase up to ~70% at 550 nm wavelength, and it is relatively fixed from 500 to 1000 nm wavelengths. Meanwhile, the sheet resistance was decreased from 454 to 135 Ω/sq.. Therefore, bi-layer structure could promote the optical and electrical property.

The optical transmittance of the PET/ZrCu/ITO is shown in Fig. 2, as a function of TFMG thickness. The transmittance of the pure single-layer ITO film is ~83% in the visible wavelength of 550 nm. The ZrCu/ITO films show the similar variation trend in transmittance as the pure ITO film in the measured spectrum, but the transmittance would decline with increasing amorphous ZrCu layer thickness, as shown in Fig. 2. The transmittance of ZrCu/ITO films with 3 nm thickness of ZrCu layer is ~75% at 550 nm wavelength. Transmittance (at 550 nm) and sheet resistance for the TFMG and TFMG/ITO films showed in Table 2. It is apparent that fix at the same sheet resistance of 136 Ω/sq., the transmittance of the PET/AgMgAl/ITO film is better than that of the PET/ZrCu/ITO film. Therefore, the transmittance could be enhanced by adjusting the TFMGs alloy system.

When the PET/ZrCu/ITO hybrid structure is subject to bending fatigue loading, micro-cracks and defects would be induced, and the in-situ measured electric resistivity would exhibit scattering and degradation with increasing fatigue cycles. Fig. 3 shows that the relative changes of resistivity as a function of the bending cycles of the PET substrate coated with either only ITO film or with the ZrCu/ITO (also simplified as the ZCI in the plot) compound films under the maximum bending curvature of 19.5 and 16.5 mm. With a lower curvature, the maximum bending fatigue strain would certainly be higher. We denote the relative changes of electrical resistivity as $\Delta R/R0$ (R0 is the initial resistivity, R is the measured resistivity after bending test and ΔR is expressed as $R-R0$). It is apparent that there would induce a higher degree of micro-cracks, and in-turns a higher degree of

electrical resistivity change ΔR/R0 with decreasing bending curvature (i.e., increasing fatigue maximum strain) and increasing fatigue cycles. Especially, a fairly stable electrical property of the ZCI compound film on the PET substrate was obtained during fatigue loading, as compared to the ITO film. The relative change of resistivity ΔR/R0 is below 0.4 for ZCI and over 0.9 for ITO.

When the bending curvature is further increased to 15.5 mm (0.40% strain per bending cycle), the maximum ΔR/R0 would reach 2.0 ZCI and 2.5 for ITO. Fig. 4 shows that SEM images of the PET/ITO and PET/ZrCu/ITO films after the bending fatigue test. The PET/ITO film after the 1,000 cycles bending fatigue test with the 15.5 mm curvature radius is shown in Fig. 4(a). It can be seen that many long and continuous cracks are already seen after only 1,000 cycles. In contrast, Fig. 4(b) shows the PET/ZrCu/ITO hybrid foil after the 10,000 long-termed bending fatigue test with the same 15.5 mm curvature radius. The cracks in PET/ ZrCu/ITO are still discontinuous. It is apparent that with the TFMG ZrCu interlayer in between PET and ITO, the long-termed fatigue resistance would be greatly enhanced.

Conclusion

The bi-layer structure consisting of a metallic glass film and an outer ITO layer can be a promising candidate for the transparent conductive film deposited on a PET flexible substrate due to the better sheet resistance of 135 Ω/sq and the transmittance of 70% at 550 nm wavelength. By adjusting the TFMGs alloy system, the optical and electrical property could be promoted. In addition, it is demonstrated that, the bi-layer structure under long-termed bending fatigue, the induced micro-cracks can be appreciably reduced, the service cycling fatigue performance can be pronouncedly improved, and a fairly stable electrical property can result in. The relative change of resistivity is below 0.4, significantly lower than the commercial PET/ITO product. The TFMG interlayer can be highly promising for the bending fatigue property.

Acknowledgement

The authors gratefully acknowledge the sponsorship from National Science Council of Taiwan under the projects No. NSC101-2120-M-110-007 and NSC102-2120-M-110-006.

Table 1 Detail sputtering parameters for film depositions

	ITO film			TFMG film		
	ITO target	Zr target	Cu target	Ag target	Mg target	Al target
Base pressure (Torr)	$9x10^{-6}$	$9x10^{-6}$	$9x10^{-6}$	$5x10^{-7}$	$5x10^{-7}$	$5x10^{-7}$
Working pressure (Torr)	$8x10^{-3}$	$4x10^{-3}$	$4x10^{-3}$	$3x10^{-3}$	$3x10^{-3}$	$3x10^{-3}$
Ar flow rate (sccm)	50	30	30	25	25	25
Discharge power (W)	150	140	84	20	100	70

Table 2 Transmittance (at 550 nm) and sheet resistance for the TFMG and TFMG/ITO

	Transmittance, % at 550 nm	Sheet resistance, Ω/□
TFMG-AgMgAl 6 nm	60%	900
TFMG-AgMgAl 15 nm	48%	454
AgMgAl 15 nm/ITO 30 nm	70%	135
ZrCu 9 nm/ ITO 30 nm	53%	136

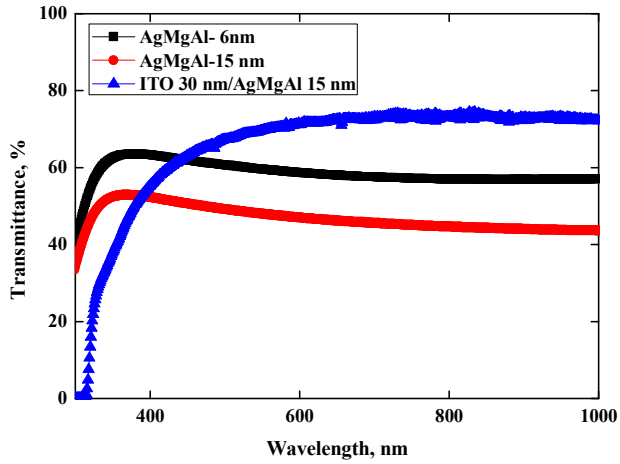

Fig. 1 The optical transmittance of the PET/TFMG-AgMgAl and PET/AgMgAl/ITO film.

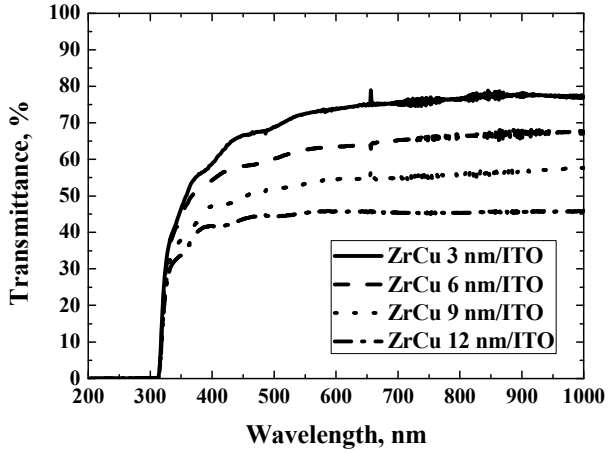

Fig. 2 The optical transmittance of ZCI films on the PET substrate as a function light wavelength for four metallic glass thicknesses from 3 to 12 nm.

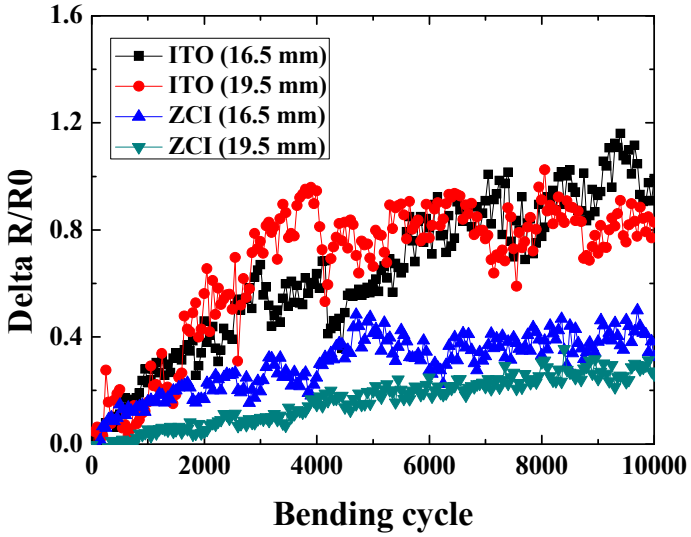

Fig. 3 The relative changes of resistivity as a function of the bending fatigue cycles of our laboratory prepared PET/ITO and PET/ZrCu/ITO with two bending curvatures of 19.5 and 16.5 mm.

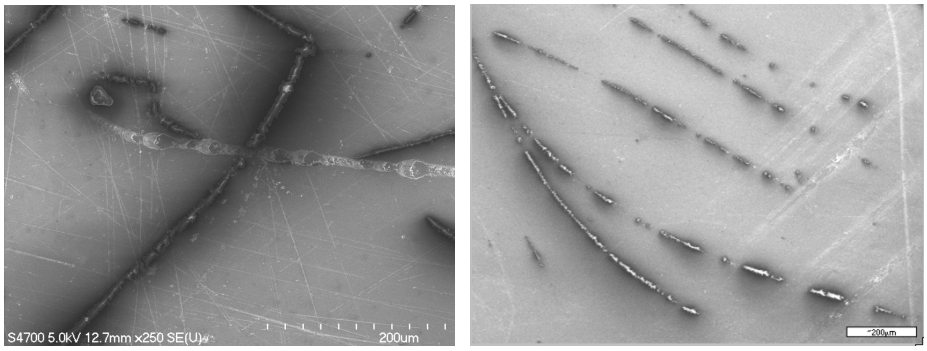

(a) (b)

Fig. 4 (a) PET/ITO after 1,000 cycles bending fatigue test with the 15.5 mm curvature radius, and (b) PET/ZrCu/ITO after 10,000 cycles bending fatigue test with the 15.5 mm curvature radius.

Reference

[1] H. Kim, C.M. Gilmore, A. Pique, J.S. Horwitz, H. Mattoussi, H. Murata, Z.H. Kafafi, D.B. Chrisey, Journal of Applied Physics, 86 (1999) 6451-6461.

[2] S.H. Cho, J.H. Park, S.C. Lee, W.S. Cho, J.H. Lee, H.H. Yon, P.K. Song, Journal of Physics and Chemistry of Solids, 69 (2008) 1334-1337.

[3] H.K. Lin, C.H. Li, S.H. Liu, Optics and Lasers in Engineering, 48 (2010) 1008-1011.

[4] C.G. Granqvist, A. Hulta˚ker, Thin Solid Films, 411 (2002) 1–5.

[5] O. J.Gregory, Q. Luo, E. E.Crisman, Thin Solid Films, 2002 (2002) 286-293.

[6] C. Guillén, J. Herrero, Thin Solid Films, 480-481 (2005) 129-132.

[7] J. Lee, H. Jung, J. Lee, D. Lim, K. Yang, J. Yi, W.-C. Song, Thin Solid Films, 516 (2008) 1634-1639.

[8] M. Bendera, W. Seeliga, C. Daubeb, H. Frankenbergerb, B. Ockerb, J. Stollenwerkb, Thin Solid Films, 326 (1998) 67–71.

[9] A. Kloppel, B. Meyer, J. Trube, Thin Solid Films, 392 (2001) 311-314.

[10] A. Indluru, T.L. Alford, Journal of Applied Physics, 105 (2009) 123528-123529.

[11] D.R. Sahu, S.-Y. Lin, J.-L. Huang, Applied Surface Science, 252 (2006) 7509-7514.

[12] M. Girtan, Solar Energy Materials and Solar Cells, 100 (2012) 153-161.
[13] X. Liu, X. Cai, J. Mao, C. Jin, Applied Surface Science, 183 (2001) 103-110.
[14] C.-W. Yang, J.-W. Park, Surface and Coatings Technology, 204 (2010) 2761-2766.
[15] D.R. Cairns, R.P. Witte Ii, D.K. Sparacin, S.M. Sachsman, D.C. Paine, G.P. Crawford, R.R. Newton, Applied Physics Letters, 76 (2000) 1425-1427.
[16] Akihisa Inoue, A. Kato, T. Zhang, S.G. Kim, T. Masumoto, Materials transactions, JIM, 32 (1991) 609-616.
[17] X.H. Du, J.C. Huang, H.M. Chen, H.S. Chou, Y.H. Lai, K.C. Hsieh, J.S.C. Jang, P.K. Liaw, Intermetallics, 17 (2009) 607-613.
[18] A. Inoue, Materials Science and Engineering, A304–306 (2001) 1–10.
[19] A. Peker, W.L. Johnson, Applied Physics Letters, 63 (1993) 2342-2344.
[20] J.P. Chu, J.C. Huang, J.S.C. Jang, Y.C. Wang, P.K. Liaw, JOM, 62 (2010) 19-24.
[21] H.S. Chou, J.C. Huang, L.W. Chang, T.G. Nieh, Applied Physics Letters, 93 (2008) 191901.
[22] J.P. Chu, J.S.C. Jang, J.C. Huang, H.S. Chou, Y. Yang, J.C. Ye, Y.C. Wang, J.W. Lee, F.X. Liu, P.K. Liaw, Y.C. Chen, C.M. Lee, C.L. Li, C. Rullyani, Thin Solid Films, 520 (2012) 5097-5122.
[23] C.J. Lee, H.K. Lin, S.Y. Sun, J.C. Huang, Applied Surface Science, 257 (2010) 239-243.